Circulation

ORIGINAL RESEARCH ARTICLE

# Genetic Lineage Tracing of Nonmyocyte Population by Dual Recombinases

Editorial, see p 806

Yan Li, PhD*
Lingjuan He, PhD*
et al

**BACKGROUND:** Whether the adult mammalian heart harbors cardiac stem cells for regeneration of cardiomyocytes is an important yet contentious topic in the field of cardiovascular regeneration. The putative myocyte stem cell populations recognized without specific cell markers, such as the cardiosphere-derived cells, or with markers such as Sca1$^+$, Bmi1$^+$, Isl1$^+$, or Abcg2$^+$ cardiac stem cells have been reported. Moreover, it remains unclear whether putative cardiac stem cells with unknown or unidentified markers exist and give rise to de novo cardiomyocytes in the adult heart.

**METHODS:** To address this question without relying on a particular stem cell marker, we developed a new genetic lineage tracing system to label all nonmyocyte populations that contain putative cardiac stem cells. Using dual lineage tracing system, we assessed whether nonmyocytes generated any new myocytes during embryonic development, during adult homeostasis, and after myocardial infarction. Skeletal muscle was also examined after injury for internal control of new myocyte generation from nonmyocytes.

**RESULTS:** By this stem cell marker–free and dual recombinases–mediated cell tracking approach, our fate mapping data show that new myocytes arise from nonmyocytes in the embryonic heart, but not in the adult heart during homeostasis or after myocardial infarction. As positive control, our lineage tracing system detected new myocytes derived from nonmyocytes in the skeletal muscle after injury.

**CONCLUSIONS:** This study provides in vivo genetic evidence for nonmyocyte to myocyte conversion in embryonic but not adult heart, arguing again the myogenic potential of putative stem cell populations for cardiac regeneration in the adult stage. This study also provides a new genetic strategy to identify endogenous stem cells, if any, in other organ systems for tissue repair and regeneration.



*Drs Yan Li and He contributed equally.

**Key Words:** cell lineage ■ myocardial infarction ■ myocardial revascularization ■ myocytes, cardiac ■ recombinases ■ stem cell

Sources of Funding, see page 803



https://www.ahajournals.org/journal/circ

## Clinical Perspective

### What Is New?

- Generation of a marker-free lineage tracing approach for nonmyocytes during homeostasis and after cardiac injuries.
- Nonmyocytes do not convert to new cardiomyocytes during adult cardiac homeostasis and myocardial infarction.
- All cardiomyocytes in injured myocardium are derived from preexisting cardiomyocytes.

### What Are the Clinical Implications?

- Our study indicates the lack of myogenic potential of putative Sca1$^+$, Bmi1$^+$, Isl1$^+$, Abcg2$^+$, or other stem cell populations for cardiac regeneration in the adult stage.
- Myocytes are the main cellular source for cardiac regeneration.
- This new genetic system provides an unprecedented strategy to readdress the contribution of putative adult stem cells to tissue repair and regeneration of multiple organ systems.

During myocardial infarction (MI) or heart attack, a large number of cardiomyocytes die after deprivation of oxygen, resulting in progression of life-threatening heart failure. Although cardiomyocytes could proliferate to generate new cardiomyocytes in the adult mammalian heart, their slow turnover rate is insufficient to compensate for the significant cell loss after MI.[1–4] Because adult cardiomyocytes rarely proliferate, identification of the endogenous cardiac stem cells (CSCs) that possess myogenic potential will provide clinical benefits for heart regeneration.[5] By definition, the endogenous CSCs are multipotent cells that can differentiate into specialized cell types of the heart, including de novo cardiomyocytes.

Recent advances appear to show that adult CSCs could differentiate into new cardiomyocytes, holding great potential in the development of cardiac regenerative medicine.[6,7] However, there is a lack of consensus on whether endogenous CSCs exist in the adult mammalian heart. For instance, the myogenic potential of c-Kit$^+$ cells remains controversial.[8–13] Ellison et al[9] reported that adult c-Kit$^+$ cells were endogenous CSCs that differentiated into new cardiomyocytes after myocardial damage, and were necessary and sufficient for functional cardiac regeneration. On the other hand, other studies indicated that c-Kit$^+$ cells minimally, if at all, contributed to new cardiomyocytes.[10–12] This refutation of c-Kit$^+$ cells as myocyte stem cells casts skepticism on the stem cell paradigm for cardiac regeneration. Whether the results from c-Kit$^+$ cell studies can be extrapolated to the cardiac stem cell field, or whether other putative CSC populations exist, remains elusive and untested.

In addition to the debate over the myogenic potential of c-Kit$^+$ stem cells, CSCs labeled by other markers, such as Sca1$^+$, Bmi1$^+$, Isl1$^+$ and ABCG2$^+$, have been proposed to give rise to cardiomyocytes for cardiac repair and regeneration.[14–17] Whether these CSCs are bona fide stem cells that generate cardiomyocytes should be readdressed rigorously by genetic lineage tracing experiments. Proving the existence of each reported CSC population requires new genetic tools that target specific promoters. Moreover, there could be other putative CSCs with unknown or unidentified molecular markers that generate new cardiomyocytes in the adult heart, such as the cardiosphere-derived cells.[18] Nevertheless, direct evidence to either support or refute the existence of endogenous CSCs is lacking, and an unequivocal conclusion on this contentious issue is important in further development of potential cardiovascular regenerative medicine.

Current research on cell fate mapping of endogenous CSCs largely relies on the conventional genetic lineage tracing technology that utilizes the promoters of specific markers expressed by CSCs. However, some proposed stem cell markers are nonspecific to putative CSCs,[12,19–21] as they are also expressed by cardiomyocytes. It remains technically challenging to trace all of the previously reported putative CSCs (eg, Bmi1, Sca1, Isl1, Abcg2, etc.) to understand their myogenic potential. In addition, conventional lineage tracing requires Cre expression under a known or characterized marker/gene promoter. However, for putative CSCs with unknown or unidentified markers, conventional lineage tracing is unable to trace them, which could hardly be overcome by the single marker–based lineage tracing platform. To trace putative CSCs without specific markers, we generated a new system that is capable of tracing all nonmyocyte populations that contain putative CSCs. This new genetic lineage tracing system is unbiased for studying new sources of cardiomyocytes, as it does not rely on a particular stem cell marker. We used this system to investigate the existence of endogenous CSCs during tissue development, during homeostasis, and after injury. The establishment of this unique tracing approach is also valuable to resolve similar questions in other organ systems.

## METHODS

Please refer to expanded methods in the online-only Data Supplement for details. The data, analytic methods, and study materials will be made available to other researchers for purposes of reproducing the results or replicating the procedure. The newly generated genetic mouse strains in this study will be available in Bin Zhou's laboratory at Chinese Academy of Sciences and the Biomodel Organism Co Ltd, Shanghai,

China. Detailed methods are provided in the online-only Data Supplement.

## Mice

The care and use of animals were in accordance with the guidelines of the Institutional Animal Care and Use Committee of the Institute of Biochemistry and Cell Biology and Institute for Nutritional Sciences, Shanghai Institutes for Biological Sciences, Chinese Academy of Sciences. The *R26-DreER*, *Isl1-CreER*, *Vim-CreER*, and *Postn-CreER* mouse lines were generated by homologous recombination using CRISPR/Cas9. Generation of *IR1*, *IR3*, *NR1*, *Tnnt2-Dre*, *Tnnt2-Cre*, *Actb-Cre*, and *Tnni3-Dre* is reported previously.[13] *R26-rtTA*, *tetO-Cre*, *aMHC-MerCreMer*, *Npr3-CreER*, *Myh11-CreER*, *Sox9-CreER*, *Pdgfrb-CreER*, *Cdh5-CreER*, *NG2-CreER*, and *Wt1-CreER* mouse lines were reported previously.[22–31]

## Immunostaining

Immunostaining was performed as according to previous protocols.[32] Briefly, hearts and other organs were collected and washed in cold PBS to remove excessive blood, and then hearts or other tissues were fixed in 4% polyformaldehyde at 4°C. After washing in PBS several times, hearts or other tissues with fluorescence reporters were observed and photographed using Zeiss stereomicroscope (Zeiss AXIO Zoom. V16). Hearts and other tissues were then dehydrated in 30% sucrose in PBS at 4°C until tissues were fully penetrated. Cryosections of tissues were then collected and blocked with PBS supplemented with 0.2% triton X-100 and 5% normal donkey serum for 30 minutes at room temperature, followed by primary antibody incubation at 4°C overnight. Detailed first antibody information including manufacturer, catalog number and dilution could be found in the online-only Data Supplement. After developing with secondary antibodies, images were acquired by Zeiss stereomicroscope (Zeiss AXIO Zoom. V16), Zeiss confocal laser scanning microscope (LSM 880), or Olympus confocal microscope (FV1000, FV1200). The image data were analyzed by ImageJ (National Institutes of Health) software.

## Statistics

Data were presented as means±standard error of the mean (SEM). No test was performed to analyze the difference between groups that contained negative data throughout this study.

# RESULTS

## Generation of a New Tracing System for Labeling Nonmyocytes

To test whether there are any putative CSCs in nonmyocytes, we generated a novel system that labels all nonmyocyte lineages. We took advantage of the exclusive dual reporter line, interleaved reporter, *IR1*,[13] in which 2 *lox*P and *rox* sites were interleaved so that either Dre-*rox* or Cre-*lox*P recombination would remove the substrate of the other recombination system, resulting in an exclusive and permanent labeling of a cell (either ZsGreen or tdTomato, Figure 1A). We will use this new system to label myocytes and nonmyocytes by 2 distinct genetic tracing markers (Figure 1A). First, we generated the *Tnnt2-Dre;R26-iCre;IR1* mouse line for labeling both cardiac troponin T (Tnnt2)$^+$ myocytes and Tnnt2$^-$ nonmyocytes: *Tnnt2-Dre* first labeled myocytes that expressed Dre; and on doxycycline (Dox) treatment, *R26-iCre* (*R26-rtTA;TRE-Cre*) then labeled all cell types except myocytes (Figure 1B). This dual tracing system allowed permanent labeling of myocytes by tdTomato and nonmyocytes by ZsGreen, respectively. We tested the specificity of this tracing system by examining individual heart sections of the *Tnnt2-Dre;IR1* mouse. Our results of immunostaining showed that tdTomato$^+$ cells were exclusively cardiomyocytes expressing the sarcomere protein troponin I (TNNI3, Figure I in the online-only Data Supplement) without expression of other lineage markers (Figure II in the online-only Data Supplement), indicating that *Tnnt2-Dre* specifically and efficiently labeled cardiomyocytes via *IR1*. To label nonmyocytes efficiently, we treated the *R26-iCre;IR1* mice with Dox at various time points. We observed labeling of almost all cells in multiple tissue sections examined (Figure III in the online-only Data Supplement) and confirmed negligible leakiness of *R26-iCre* in the absence of Dox treatment (Figure IV in the online-only Data Supplement).

We first tested the efficacy of this tracing system to examine the nonmyocyte to myocyte conversion in the embryonic heart, as nonmyocytes such as the *Isl1*$^+$ second heart field progenitors residing dorsal to the *Mlc2a*$^+$ first heart field progenitors contribute to myocytes of the right ventricle (Figure 1C).[33,34] Induction of tamoxifen at E8.0 in the *Isl1-CreER;R26-tdTomato* mouse line labeled the right ventricle at E13.5 (Figure 1D), consistent with previous findings.[33] We then injected Dox to label the nonmyocytes in the *Tnnt2-Dre;R26-iCre;IR1* mouse line at E8.0 and found the tdTomato$^+$ heart and ZsGreen$^+$ cells in other tissues at E8.5 (Figure 1E). We next collected E13.5 heart and examined the cell fate conversion of second heart field progenitors to myocytes of the right ventricle (Figure 1F). Indeed, immunostaining for tdTomato, ZsGreen, and the myocyte marker TNNI3 of E13.5 heart sections showed that the majority of myocytes in the right ventricle were ZsGreen$^+$ (Figure 1F), demonstrating that this new tracing system efficiently detect nonmyocyte to myocyte conversion in the developing heart.

## Nonmyocytes Did Not Contribute to Myocyte in the Adult Heart (Strategy 1)

We next used *Tnnt2-Dre;R26-iCre;IR1* to trace cardiomyocytes and nonmyocytes simultaneously in the adult heart. Dox treatment resulted in Cre expression ubiquitously in all types of cells (Figure 1B). Because *Tnnt2-*

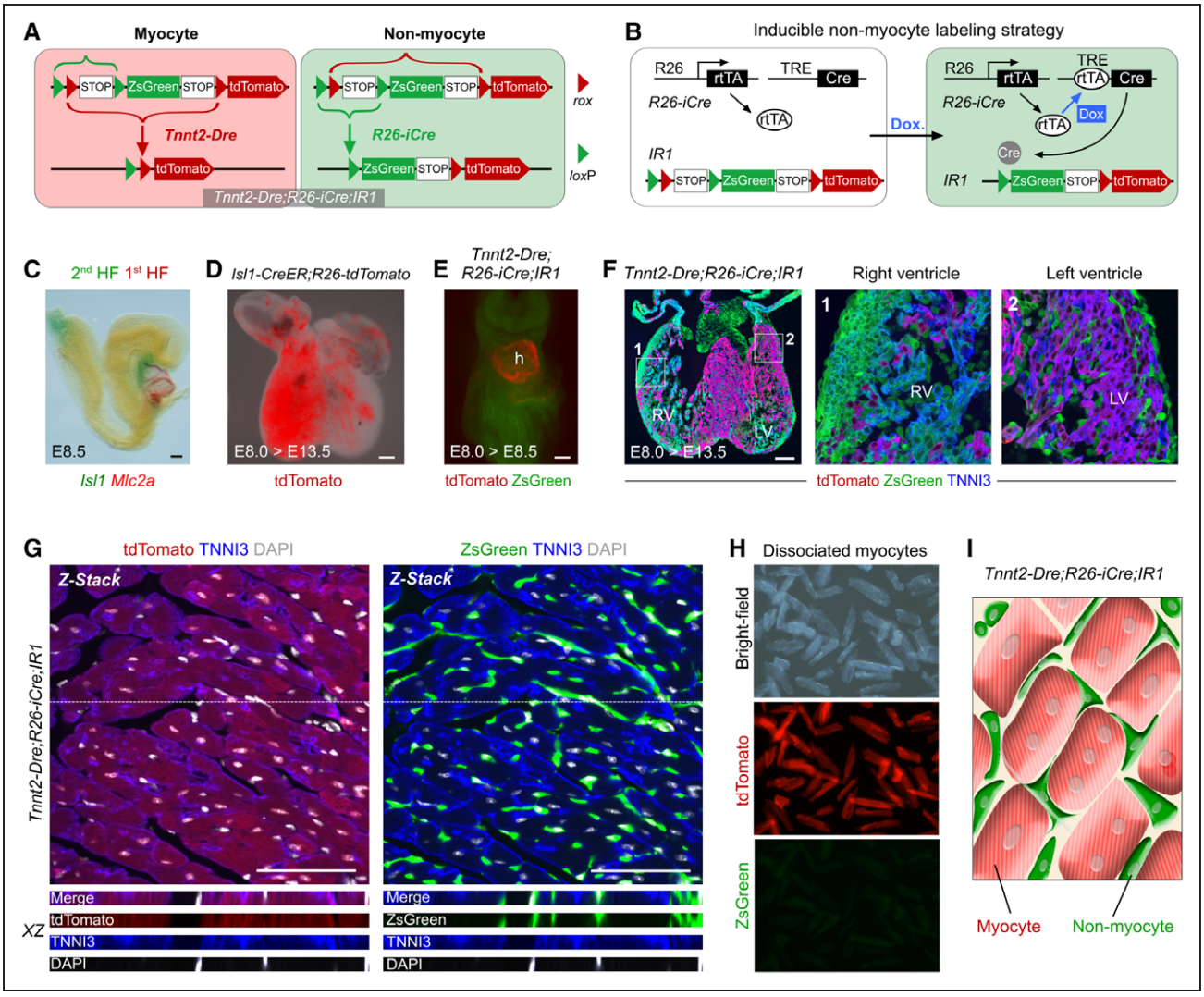


**Figure 1. Genetic labeling of nonmyocytes by *Tnnt2-Dre;R26-iCre;IR1* strategy.**
**A,** Strategy for labeling myocytes and nonmyocytes by *Tnnt2-Dre;R26-iCre;IR1*. **B,** Inducible nonmyocyte labeling by doxycycline (Dox) induced Cre-loxP recombination using *R26-iCre* (*R26-rtTA;TRE-Cre*). **C,** In situ hybridization of *Mlc2a* and *Isl1*, respectively, show 1st (red) and 2nd (green) heart fields. **D,** The Isl1+ cell lineage (tdTomato) mainly contributes to the right ventricle at E13.5 of *Isl1-CreER;R26-tdTomato*. Tamoxifen was induced at E8.0. **E,** Whole-mount epifluorescence image for E9.0 *Tnnt2-Dre;R26-iCre;IR1* embryo. Dox was induced at E8.0. h, heart. **F,** Immunostaining for tdTomato, ZsGreen, and TNNI3 on E13.5 *Tnnt2-Dre;R26-iCre;IR1* heart. Dox was induced at E8.0. LV indicates left ventricle; and RV, right ventricle. **G,** Immunostaining for tdTomato, ZsGreen, TNNI3, and DAPI on adult heart section. Tissue samples were collected 2 weeks after Dox treatment. *XZ* indicates signals from dotted lines on *Z*-stack images. Scale bars, 100 μm. **H,** Bright-field and fluorescence images of dissociated myocytes from adult mouse heart. Scale bars, 100 μm. **I,** Cartoon image showing labeling of nonmyocytes (green) and myocytes (red) distinctively by *Tnnt2-Dre;R26-iCre;IR1*.

*Dre*–mediated Dre-rox recombination labeled myocytes as tdTomato before Dox treatment, induced Cre expression in myocytes did not further label myocytes by ZsGreen (Figure 1A and 1B). Immunostaining for tdTomato, ZsGreen, and TNNI3 on adult heart sections showed that tdTomato$^+$ cells are TNNI3$^+$ cardiomyocytes, whereas ZsGreen$^+$ cells are not TNNI3$^+$ cardiomyocytes (Figure 1G). Examination of dissociated cardiomyocytes from *Tnnt2-Dre;R26-iCre;IR1* heart confirmed that there was no ZsGreen$^+$ cardiomyocyte (Figure 1H). Our system therefore labeled myocytes and nonmyocytes with two distinct genetic tracers (Figure 1I).

We next used this tracing system to test whether nonmyocytes (trans) differentiate into myocytes in the adult heart. If this happens, the new myocytes derived from nonmyocytes would be ZsGreen$^+$. After Dox treatment, we induced MI in *Tnnt2-Dre;R26-iCre;IR1* mice by ligation of left anterior descending coronary artery (Figure 2A). At 2 to 4 weeks after injury, we examined whether there was nonmyocyte to myocyte conversion in the injured hearts by immunostaining for ZsGreen, tdTomato, and TNNI3. As a control, we performed sham operation and examined heart tissues to see whether there was any ZsGreen$^+$ cardiomyocyte. Immunostaining for tdTomato, ZsGreen, and TNNI3 on heart sections showed that there was no ZsGreen$^+$TNNI3$^+$ cardiomyocyte (Figure 2B). We next examined the MI tissue to see whether cardiac injury unlocks the myogenic potential

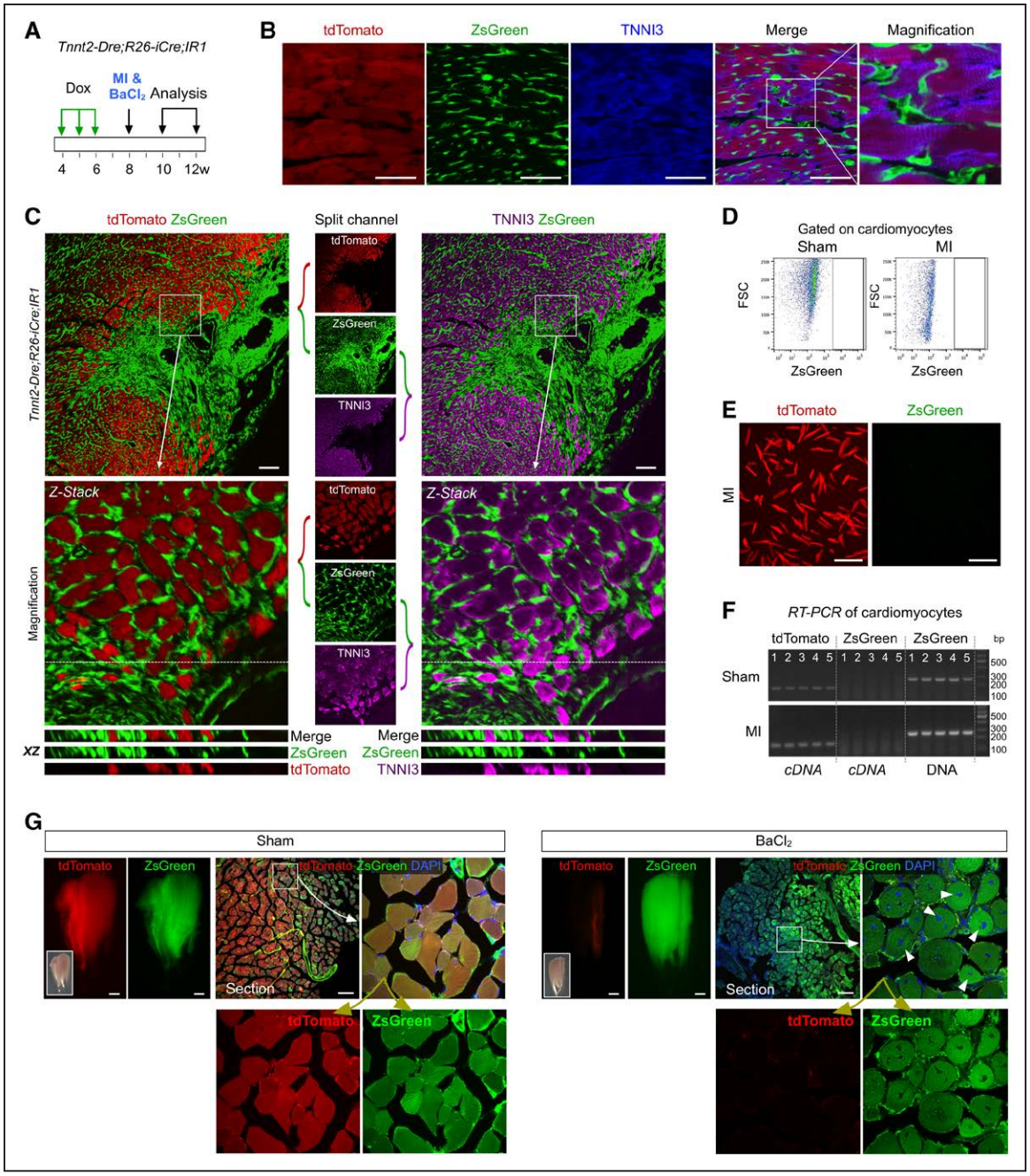


**Figure 2. Analysis of nonmyocyte to myocyte conversion by *Tnnt2-Dre;R26-iCre;IR1* strategy.**
**A,** Schematic figure showing experimental procedures. **B,** Immunostaining for tdTomato, ZsGreen, and TNNI3 on sham heart section. **C,** Immunostaining for tdTomato, ZsGreen, and TNNI3 on MI heart sections. *XZ* indicates signals from dotted lines on *Z*-stack images. **D,** Flow cytometric analysis of cardiomyocytes isolated from sham or MI hearts. **E,** Fluorescence images of dissociated cardiomyocytes from MI heart. **F,** Reverse transcription–polymerase chain reaction (RT-PCR) of ZsGreen or tdTomato in dissociated cardiomyocytes. DNA is included as positive control for ZsGreen PCR;1 to 5 are 5 tissue samples. **G,** Whole-mount fluorescence images of TA muscle and immunostaining for tdTomato and ZsGreen on sections of sham or $BaCl_2$-treated muscles. Arrowheads indicate ZsGreen$^+$tdTomato$^-$ new myocytes. Insets are bright-field images. Scale bars, 1 mm in **G** (whole-mount pictures); 100 μm in others. Each image is a representative of 5 individual samples.

of nonmyocytes. In the infarcted myocardium, we did not detect a single ZsGreen$^+$tdTomato$^-$ cardiomyocyte after examination of >600 sections from 5 *Tnnt2-Dre;R26-iCre;IR1* hearts (Figure 2C). We also confirmed by flow cytometry (Figure 2D) and fluorescent microscopy (Figure 2E) that no ZsGreen$^+$ cardiomyocyte could be observed in the dissociated cardiomyocytes of MI hearts of the *Tnnt2-Dre;R26-iCre;IR1* mice. Moreover, reverse transcription–polymerase chain reaction (RT-PCR) of the dissociated cardiomyocytes showed mRNA expression of *tdTomato* but not *ZsGreen* (n=5, Figure 2F). Our data indicated that nonmyocytes did not contribute to myocytes after cardiac injury in the adult heart.

We also examined the cell fate conversion of nonmyocytes to myocytes in skeletal muscle after injury that served as a positive control for our experiments.

In the normal skeletal muscle (sham), we detected tdTomato+ZsGreen+ myocytes (Figure 2G), which could be attributable to cell fusion of nonmyocytes and myocytes in skeletal muscle. We performed $BaCl_2$ injection into the tibial anterior (TA) muscle of *Tnnt2-Dre;R26-iCre;IR1* limbs. Whole-mount fluorescence view of TA muscle showed weak tdTomato and strong ZsGreen expression after injury, indicating ablation of tdTomato+ myocytes after $BaCl_2$ treatment and subsequent replacement by ZsGreen+ cells (Figure 2G). In the injured TA muscle, we detected ZsGreen+tdTomato− myocytes (arrowheads, Figure 2G) compared with the sham-operated group, indicating de novo formation of myocytes from nonmyocytes. Taken together, dual lineage tracing by *Tnnt2-Dre;R26-iCre;IR1* (Strategy 1) revealed the nonmyocyte to myocyte conversion in the embryonic heart and adult skeletal muscle, but not in the adult heart.

## Reverse of Cre/Dre System for Labeling cells in the Study of Nonmyocyte to Myocyte Conversion (Strategy 2)

To independently validate nonmyocyte to myocyte conversion, we generated a second dual tracing system which consisted of *Tnnt2-Cre*, a transgenic line that expressed Cre in myocytes,[35] tamoxifen inducible *R26-DreER*, and an alternative interleaved reporter *IR3*.[13] With *IR3*, we could exclusively label myocytes by ZsGreen and nonmyocytes by tdTomato (Figure 3A). *R26-DreER;IR3* efficiently labeled the majority of cells in the organs examined after tamoxifen treatment (Figure VA in the online-only Data Supplement), consistent with the ubiquitously active nature of Rosa26 locus.[36] There was sparse labeling in *R26-DreER;IR3* tissues without tamoxifen treatment (Figure VI in the online-only Data Supplement), suggesting negligible leakiness. We next generated the *Tnnt2-Cre;R26-DreER;IR3* mouse line to simultaneously label myocytes and nonmyocytes (Figure 3A). Examination of the E8.0 embryonic heart revealed ZsGreen labeling of the primary heart tube at E8.0 (Figure 3B). Following tamoxifen induction at E8.0, a significant contribution of tdTomato+ nonmyocytes to myocytes was found at E13.5 in the right ventricle (Figure 3C). Immunostaining on heart sections also confirmed contribution of nonmyocytes to myocytes in the right ventricle (Figure 3D–3F). Similarly, in the adult heart and skeletal muscle, we examined cell fate conversion of nonmyocytes after MI and $BaCl_2$ treatment, respectively (Figure 3G). The nonmyocytes in *Tnnt2-Cre;R26-DreER;IR3* mouse heart were efficiently labeled (Figure VB in the online-only Data Supplement). Flow cytometric analysis (Figure 3H) and fluorescence microscopy (Figure 3I) of dissociated cardiomyocytes, respectively, showed that there was no tdTomato+ cardiomyocyte. Morphologically, these tdTomato+ cells were distinct from ZsGreen+ cardiomyocytes (Figure 3J). Immunostaining for tdTomato and TNNI3 showed that these tdTomato+ cells did not give rise to TNNI3+ cardiomyocytes in the infarcted, border, and remote zones of MI hearts (Figure 3K). No tdTomato+TNNI3+ cardiomyocyte was detected after examination of >600 tissue sections from 5 *Tnnt2-Cre;R26-DreER;IR3* hearts. By RT-PCR, we detected *ZsGreen* but not *tdTomato* mRNA from the dissociated cardiomyocytes (Figure 3L). In contrast, we could readily detect tdTomato+ZsGreen− myocytes in the injured TA muscle collected from the same mouse treated with tamoxifen (arrowheads, Figure 3M), but not from the sham-operated group. The myocytes in sham group were tdTomato+ZsGreen+ as a result of cell fusion of nonmyocytes and myocytes in the skeletal muscle. Taken together, our results of dual lineage tracing by *Tnnt2-Cre;R26-DreER;IR3* also revealed nonmyocyte to myocyte conversion in the embryonic heart and adult skeletal muscle, but not in the adult heart.

## Nonmyocyte to Myocyte Conversion Examined by *Tnnt3-Dre;R26-iCre;IR1* System (Strategy 3)

To further validate the above findings, we used an additional myocyte marker TNNI3 to drive Dre recombinase. *Tnni3-Dre* efficiently and specifically labeled myocytes but not nonmyocytes in the adult heart (Figure VII in the online-only Data Supplement). We generated the *Tnni3-Dre;R26-iCre;IR1* mouse line to distinctively label myocytes and nonmyocytes (Figure 4A). Immunostaining for ZsGreen, tdTomato, and different cardiac cell lineage markers showed tdTomato expression in myocytes and ZsGreen expression in nonmyocytes (Figure VIII in the online-only Data Supplement). *R26-iCre* efficiently labeled nonmyocytes such as endothelial cells, pericytes, fibroblasts, et al. (Figure VIII in the online-only Data Supplement). Without Dox treatment, no ZsGreen+ cell was observed in the *Tnni3-Dre;R26-iCre;IR1* mouse tissues (Figure 4B). Two weeks after Dox treatment, we performed MI or $BaCl_2$ treatment to examine whether nonmyocyte to myocyte conversion was possible following cardiac or skeletal muscle injury (Figure 4C). In the sham-operated hearts, Dox treatment led to ZsGreen labeling of cardiac cells, in addition to tdTomato+ myocytes (Figure 4D). Immunostaining for tdTomato, ZsGreen, and TNNI3 showed that all cardiomyocytes were tdTomato+ ZsGreen- (Figure 4E). After MI, there was a significant reduction in the number of tdTomato+ myocytes in the infarcted region replaced by ZsGreen+ nonmyocytes (Figure 4F). The dissociated cardiomyocytes from MI heart were tdTomato+ZsGreen− (Figure 4G). Immunostaining for tdTomato, ZsGreen, and TNNI3 on MI heart sections showed that ZsGreen+ cells did not adopt the cardiomyocyte lineage after injury

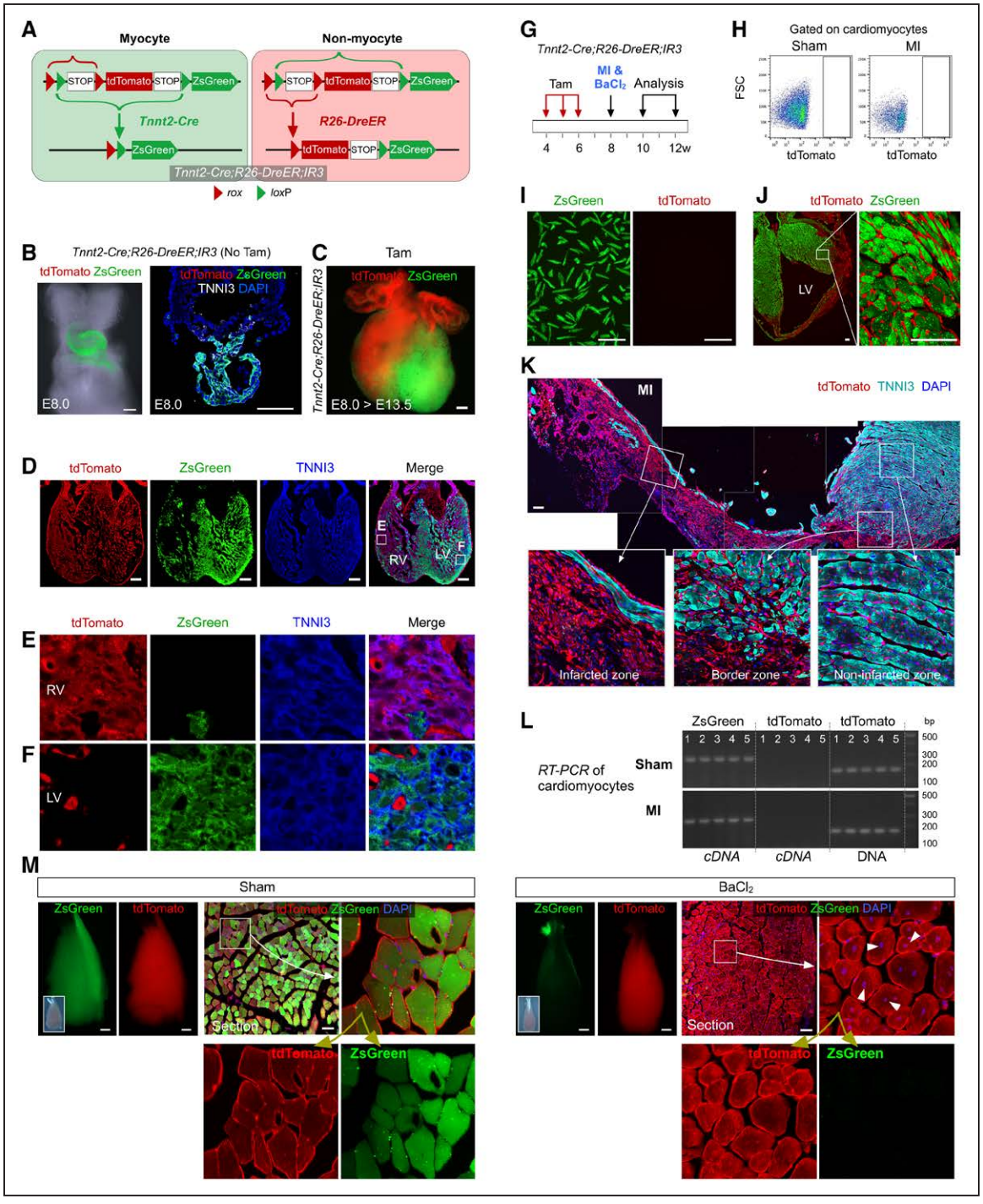


**Figure 3. New myocytes derived from nonmyocytes in the embryonic but not the adult heart.**
**A,** Schematic figure showing Cre-loxP recombination in myocytes and Dre-rox recombination in nonmyocytes by *Tnnt2-Cre;R26-DreER;IR3* strategy. **B,** Whole-mount and section view of E8.0 *Tnnt2-Cre;R26-DreER;IR3* heart without tamoxifen treatment. **C,** Whole-mount fluorescence view of E13.5 *Tnnt2-Cre;R26-DreER;IR3* heart after tamoxifen treatment at E8.0. **D** through **F,** Immunostaining for tdTomato, ZsGreen, and TNNI3 on heart sections from **C**. Boxed regions in **D** are magnified in **E** and **F**. **G,** Experimental strategy for adult heart study by myocardial infarction (MI), and skeletal muscle by $BaCl_2$ treatment. **H,** Flow cytometric analysis of isolated cardiomyocytes from sham or MI heart. **I,** Image of dissociated cardiomyocytes from MI heart. **J,** Immunostaining for tdTomato and ZsGreen on MI heart section. **K,** Immunostaining for tdTomato and TNNI3 on MI heart sections. **L,** RT-PCR analysis of ZsGreen or tdTomato cDNA of cardiomyocytes. DNA is included as positive control for tdTomato; 1 to 5 are 5 tissue samples. **M,** Whole-mount fluorescence images of TA muscle and immunostaining for tdTomato and ZsGreen on sections of sham or $BaCl_2$ treated muscles. Arrowheads indicate $tdTomato^+ZsGreen^-$ myocytes. Insets are bright-field images. Scale bars, 1 mm in **M** (whole-mount pictures); 100 μm in others. Each image is a representative of 5 individual samples.

(Figure 4H and 4I). By flow cytometric analysis and RT-PCR with dissociated myocytes, respectively, we did not detect any $ZsGreen^+tdTomato^-$ myocyte in the MI heart (Figure 4J and 4K). In contrast, we detected $ZsGreen^+tdTomato^-$ myocytes in the injured TA muscle (arrowheads, Figure 4L), indicating de novo gen-

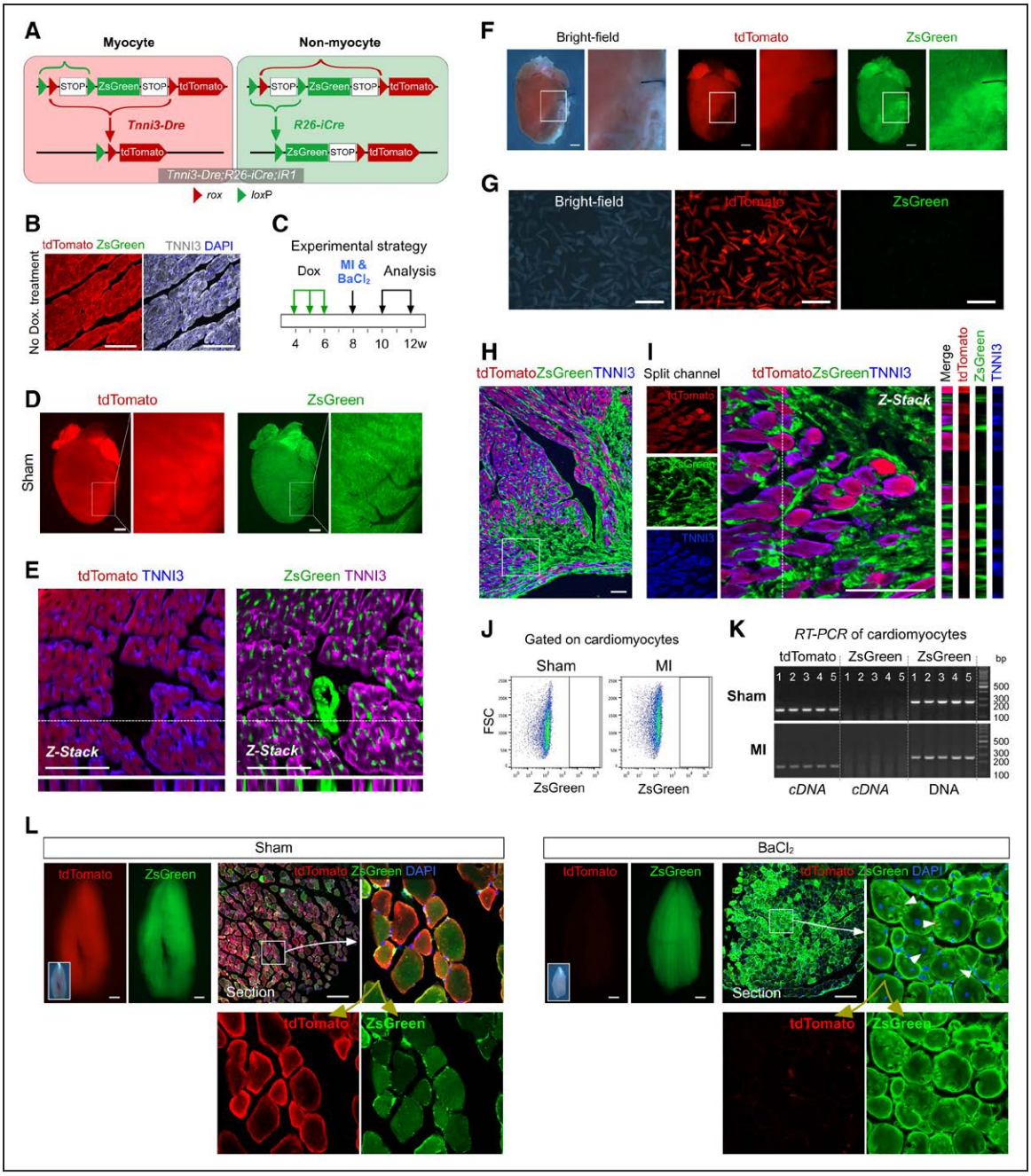


**Figure 4. Nonmyocyte to myocyte conversion detected by *Tnni3-Dre;R26-iCre;IR1* strategy.**
**A,** Schematic figure showing labeling strategy for myocytes and nonmyocytes. **B,** Immunostaining for tdTomato, ZsGreen, and TNNI3 on heart sections of mouse without Dox treatment. **C,** Schematic figure showing experimental strategy. **D,** Whole-mount fluorescence view of sham heart. **E,** Immunostaining for tdTomato, ZsGreen, and TNNI3 on sham heart section. **F,** Whole-mount fluorescence views of MI hearts. **G,** Fluorescence images of isolated cardiomyocytes. **H** and **I,** Immunostaining for tdTomato, ZsGreen, and TNNI3 on MI heart section. Boxed region in **H** is magnified in **I**. **J,** Flow cytometric analysis of dissociated cardiomyocytes. **K,** Reverse transcription–polymerase chain reaction (RT-PCR) of genes in isolated cardiomyocytes. **L,** Whole-mount fluorescence images of TA muscle and immunostaining for tdTomato and ZsGreen on sections of sham or $BaCl_2$-treated muscles. Arrowheads indicate $ZsGreen^+tdTomato^-$ new myocytes. Scale bars, 1 mm in **F**, **G**, and **L**, whole-mount tissues; 100 μm in others. Each image is a representative of 5 individual samples.

eration of myocytes from nonmyocytes. In the normal skeletal muscle, myocytes were $tdTomato^+ZsGreen^+$ as a result of cell fusion of nonmyoyctes and myocytes. Taken together, this third lineage tracing model based on *Tnni3-Dre;R26-iCre;IR1* independently revealed that there was no nonmyocyte to myocyte conversion in the adult heart.

## Nonmyocyte to Myocyte Conversion Examined by *NR1* System (Strategy 4)

Although our inducible Cre or Dre under the control of ubiquitous promoter was efficient in labeling the majority of nonmyocytes, we observed that the labeling efficiency was not reaching 100%. It is possible but less

likely that the few unlabeled nonmyocytes generated new myocytes in the adult heart after injury because the labeling process was random during lineage tracing. To achieve 100% labeling efficiency of nonmyocytes, we developed the fourth strategy to label all mouse cells by ZsGreen, except for newly-formed myocytes which were labeled by tdTomato (Figure 5A). This was achieved by using the nested reporter 1, *NR1*,[13] in which all cells in the mouse were first labeled as ZsGreen after *Actb-Cre-lox*P recombination. Only new myocytes, when formed, would switch on tdTomato after a secondary *Tnnt2-Dre-rox* recombination (Figure 5A). Although the Dre-rox recombination in myocytes led to tdTomato expression, the ZsGreen protein was still stable for labeling with extra time before degradation because the green fluorescent protein has a half-life of 12 to 24 hours in mammalian cells.[37] Therefore, we expected that double positive cells could be detected during nonmyocyte to myocyte conversion (Figure 5A). To test this, we first analyzed the embryonic heart as previously demonstrated (Figure 5B). Indeed, we readily detected tdTomato$^+$ZsGreen$^+$ myocytes in the outflow tract of the E8.5 developing heart (arrowheads, Figure 5C), consistent with previous work that showed the second heart field progenitors differentiate into cardiomyocytes at this stage.[33] We then performed analysis of the adult heart by collecting heart samples at a 12-hour interval from 12 hours to 28 days after MI (Figure 5B). Immunostaining for ZsGreen, tdTomato, and TNNI3 showed no single ZsGreen$^+$tdTomato$^+$ myocyte in the infarcted myocardium (Figure 5D). For all these 56 time points, we did not detect any ZsGreen$^+$tdtomato$^+$ myocyte in >6000 heart sections from *Tnnt2-Dre;Actb-Cre;NR1* mouse hearts. Similarly, flow cytometric analysis of dissociated cardiomyocytes showed no myocytes emerged from ZsGreen$^+$ cells (Figure 5E). In contrast, we readily detected ZsGreen$^+$tdTomato$^+$ myocytes in the injured TA muscle (Figure 5F). The labeling percentage of ZsGreen in nonmyocyte lineages were 100% in the *Tnnt2-Dre;Actb-Cre;NR1* mouse heart sections (Figure IX in the online-only Data Supplement). Taken together, our results using the fourth lineage tracing strategy based on *Tnnt2-Dre;Actb-Cre;NR1* revealed that nonmyocyte to myocyte conversion could only be found in the embryonic but not the adult heart.

## Myocyte Contribution From Different Cardiac Cell Lineages

In addition to cardiomyocytes in the adult heart, there are multiple nonmyocyte cell lineages with known molecular markers (Figure XA in the online-only Data Supplement). For these different cell populations, we used conventional Cre drivers under the control of different promoters such as endocardial cells, *Npr3-CreER*;[25] mesenchymal stromal cells or fibroblast cell lineages *Sox9-CreER*,[27] *Vim-CreER*, and *Postn-CreER* (newly generated); endothelial cells, *Cdh5-CreER*;[29] pericytes or smooth muscle cells, *Myh11-CreER*,[26] *Pdgfrb-CreER*,[28] *NG2-CreER*;[30] epicardial cells, *Wt1-CreER*[31] to trace for the cell fate of nonmyocytes. As a control, we also included cardiomyocyte Cre line *aMHC-MerCreMer*, *aMHC-MCM*[24] to trace cardiomyocytes. We treated these 10 mouse lines with tamoxifen and performed MI or sham operation 2 weeks afterward, and collected samples 4 weeks later after cardiac injury (Figure XB in the online-only Data Supplement). Immunostaining for genetic marker tdTomato with cardiomyocyte marker TNNI3 on heart sections of these 10 mouse lines showed that there was no myocyte contribution from these different cell lineages after sham or MI except from preexisting cardiomyocytes (Figure XC and XD in the online-only Data Supplement). Our results indicated that all these nonmyocytes did not contribute to new myocytes, although the *aMHC-MerCreMer* tracing data showed that virtually all myocytes in the injured heart were derived from preexisting myocytes (Figure XC and XD in the online-only Data Supplement). Therefore, our results supported the myocyte-to-myocyte, but not the nonmyocyte to myocyte conversion model in cardiac regeneration.

# DISCUSSION

In this study, we used a newly developed tracing technology to address whether endogenous CSCs exist in the developing and adult hearts. By 4 independent lineage tracing strategies, we provided direct genetic evidence that contribution of putative stem cells to myocytes only happens in the embryonic but not in the adult heart (Figure 5G), raising caution on the existence of adult CSCs during homeostasis and after injury. For the first 2 strategies, we used interleaved reporter lines (*IR1* or *IR3*) to distinctively label myocytes and nonmyocytes. To ensure specific and efficient labeling of myocytes, we used multiple constitutively active recombinase drivers under cardiac promoters such as TNNI3 and TNNT2. For induced labeling of nonmyocytes, we adopted 2 different induction strategies via Dox or tamoxifen treatment. Because the interleaved reporter determines that the labeling of myocytes and nonmyocytes by 2 distinct reporters is permanent and irreversible, any new myocyte derived from nonmyocyte would be detected by their genetic labeling if this process does happen. With results from these different strategies, we did not detect any new myocyte derived from nonmyocyte after injury. Because the inducible labeling of nonmyocytes was not 100%, we adopted the fourth strategy using the nested reporter. If nonmyocyte differentiates into myocyte, the protein of ZsGreen and tdTomato could be detected in the same cell during the transitional period. However,

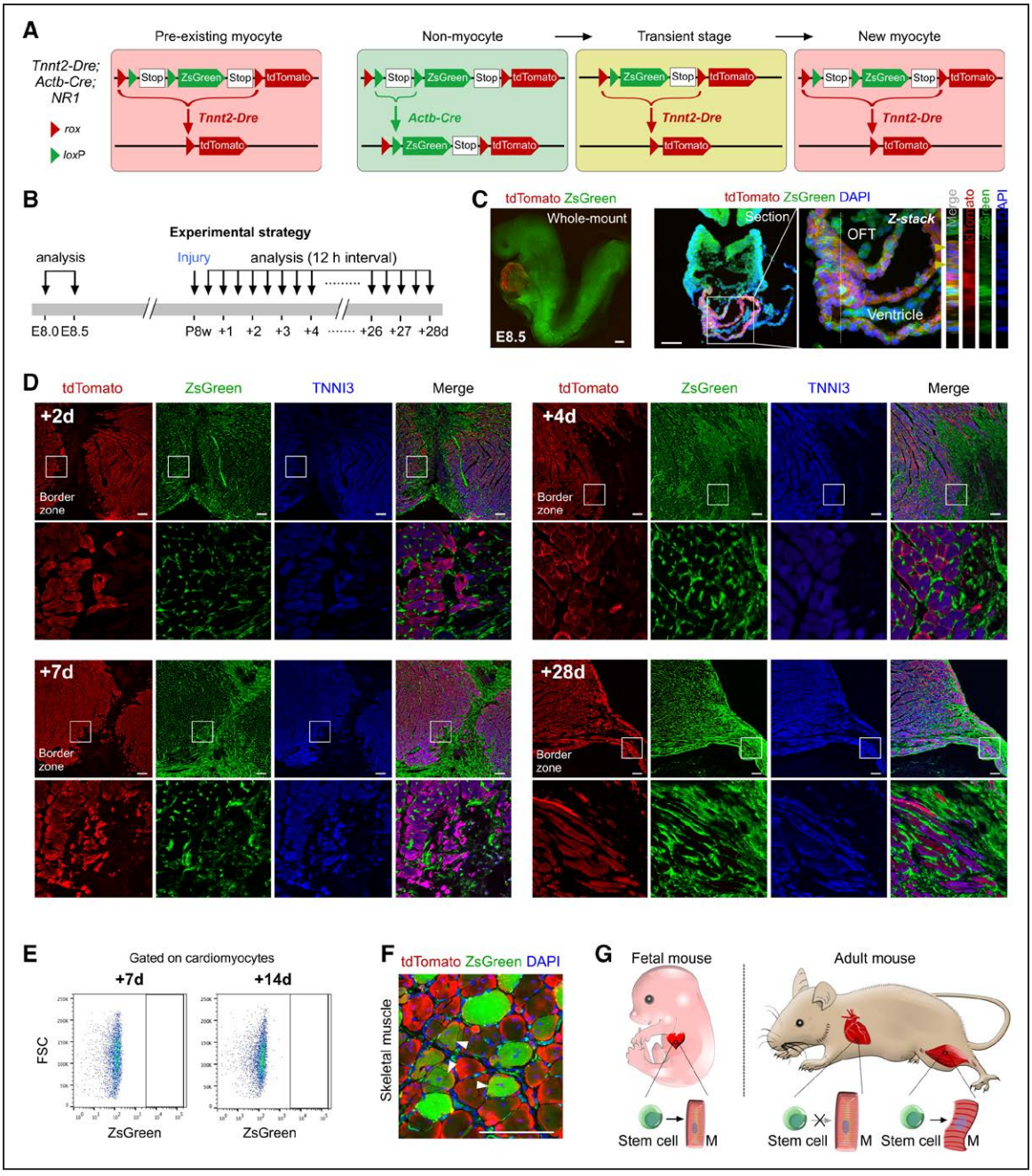


**Figure 5. Nonmyocyte to myocyte transition examined by *Tnnt2-Dre;Actb-Cre;NR1* strategy.**
**A,** Schematic figure showing lineage tracing strategy using *Tnnt2-Dre;Actb-Cre;NR1* mouse. When ZsGreen$^+$ nonmyocyte turns into myocyte, Dre-rox recombination leads to tdTomato expression. Both tdTomato and remaining ZsGreen protein will be detected during cell fate conversion. **B,** Experimental strategy for injury and analysis of *Tnnt2-Dre;Actb-Cre;NR1* mouse or embryos. **C,** Whole-mount and sectional staining of the E8.5 embryo. Arrowheads indicate tdTomato$^+$ZsGreen$^+$ cardiomyocytes in the outflow tract (OFT). **D,** Immunostaining for tdTomato, ZsGreen, and TNNI3 on adult heart sections at the indicated time points after injury. **E,** Flow cytometric analysis of cardiomyocytes collected from MI hearts. **F,** Immunostaining for tdTomato and ZsGreen from skeletal muscle shows tdTomato$^+$ZsGreen$^+$ myocytes (arrowheads) after $BaCl_2$-induced injury. **G,** Cartoon image showing myocytes (M) derived from putative stem cells in fetal heart or adult skeletal muscle, but not in the adult mouse heart. Scale bars, 100 μm. Each image is a representative of 2 individual samples.

we did not detect any double positive cell from 12 hours to 28 days after MI, indicating no conversion of nonmyocyte to myocyte after cardiac injury.

We also included several controls for detection of nonmyocyte to myocyte conversion in vivo. By using both interleaved and nested reporter lines, we found contribution of stem cells to cardiomyocytes in the developing heart, demonstrating that nonmyocyte to myocyte conversion was detected by our new systems, consistent with the previous study.[33] In addition to the embryonic heart, we also included an additional positive control that showed nonmyocytes contributed to myocytes in adult skeletal muscle of the same mouse after injury (Figure 5G). Taken together, similar to neo-

natal heart regeneration in mammals, our work suggested that new cardiomyocytes in injured myocardium of the adult mouse heart were derived from preexisting cardiomyocytes, and mammalian cardiac regeneration was not mediated by de novo differentiation of endogenous CSCs in the adult stage. This myocyte to myocyte regeneration model is also evolutionally conserved as evidenced by heart regeneration in lower vertebrates including the adult zebrafish.[38,39] In the future, it is important to unravel mechanisms for driving cardiac regeneration in the adult heart including facilitated replication of preexisting cardiomyocytes[2,4] or forced expression of exogenous cardiomyocyte reprogramming factors.[40–42] Nevertheless, our novel lineage tracing system used in this study provided direct genetic evidence that endogenous CSCs exist in fetal but not in adult heart.

Our model also offered an unprecedented strategy to readdress the contribution of putative adult stem cells in tissue repair and regeneration of other organ systems. Indeed, it is still controversial whether adult stem cells or progenitor cells exist to regenerate other organs including hepatocytes of the liver,[43,44] β-cells of the pancreas,[45,46] or mammary tissues.[47,48] Our new system could be a valuable tool to readdress this issue without the use of known molecular markers for lineage tracing of stem/progenitor cells that sometimes are nonspecific or controversial. This stem cell marker–independent approach could also be widely applicable to stem cell study in other organ systems. Furthermore, this system can also be used as a novel reporter system to study reprogramming or transdifferentiation of nonparachymal cells to parachymal cells in vivo, and to investigate cell fusion in vivo without the need of cell transplantation.[49,50] Altogether, the dual tracing system reported here will provide a more sophisticated and precise genetic lineage tracing strategy for mapping cell fate in development, diseases, and regeneration.[13]

## Conclusions

Without addressing putative myocyte stem cell populations individually, this study used marker-free lineage tracing strategy and provided evidence of nonmyocyte to myocyte differentiation in embryonic but not adult mammalian heart in either cardiac homeostasis or after myocardial infarction. This work also provides a unique system for studying the putative resident stem cells in other organs during development and tissue regeneration.

## ARTICLE INFORMATION

Received February 8, 2018; accepted April 9, 2018.

The online-only Data Supplement is available with this article at https://www.ahajournals.org/doi/suppl/10.1161/CIRCULATIONAHA.118.034250.

### Authors

Yan Li, PhD*; Lingjuan He, PhD*; Xiuzhen Huang, BS; Shirin Issa Bhaloo, PhD; Huan Zhao, BS; Shaohua Zhang, BS; Wenjuan Pu, BS; Xueying Tian, PhD; Yi Li, BS; Qiaozhen Liu, PhD; Wei Yu, PhD; Libo Zhang, BS; Xiuxiu Liu, BS; Kuo Liu, BS; Juan Tang, PhD; Hui Zhang, PhD; Dongqing Cai, PhD; Adams H. Ralf, PhD; Qingbo Xu, PhD; Kathy O. Lui, PhD; Bin Zhou, MD, PhD

### Correspondence

Bin Zhou, MD, PhD, Chinese Academy of Sciences, 320 Yueyang Road, A2112, Shanghai, 200031, China. E-mail zhoubin@sibs.ac.cn

### Affiliations

The State Key Laboratory of Cell Biology, CAS Center for Excellence in Molecular Cell Science, Shanghai Institute of Biochemistry and Cell Biology, and Key Laboratory of Nutrition and Metabolism, Institute for Nutritional Sciences, Shanghai Institutes for Biological Sciences, Chinese Academy of Sciences, University of Chinese Academy of Sciences, China (Yan Li, L.H., X.H., H.Z., S.Z., W.P., X.T., Yi Li, Q.L., W.Y., L.Z., X.L., K.L., J.T., H.Z., B.Z.). Cardiovascular Division, British Heart Foundation Centre, King's College London, United Kingdom (S.I.B. Q.X.). School of Life Science and Technology, ShanghaiTech University, China (B.Z.). Key Laboratory of Regenerative Medicine of Ministry of Education, Jinan University, China (X.T., D.C., B.Z.). Max Planck Institute for Molecular Biomedicine, Department of Tissue Morphogenesis, Faculty of Medicine, University of Muenster, Germany (A.H.R.). Department of Chemical Pathology, Li Ka Shing Institute of Health Sciences, The Chinese University of Hong Kong, Prince of Wales Hospital, Shatin, Hong Kong SAR, China (K.O.L.).

### Acknowledgments

The authors thank Shanghai Biomodel Organism Co Ltd and Nanjing Biomedical Research Institute of Nanjing University for mouse generation. The authors appreciate the valuable comments and suggestions from William Pu, Paul Riley, and Ritu Dhand. The authors also thank Baojin Wu, Guoyuan Chen, Zhonghui Weng, and Aimin Huang for the animal husbandry, Wei Bian for technical help, and the National Center for Protein Science Shanghai for helping in confocal imaging.

### Sources of Funding

This work was supported by the Strategic Priority Research Program of the Chinese Academy of Sciences (CAS, XDB19000000, XDA16020204), National Science Foundation of China (31730112, 91639302, 31625019, 81761138040, 31571503, 31501172, 31601168, 31701292, 91749122), National key Research & Development Program of China (SQ2018YFA010021, SQ2018YFA010113, 2016YFC1300600 and 2017YFC1001303), Youth Innovation Promotion Association of CAS (2015218, 2060299), Key Project of Frontier Sciences of CAS (QYZDB-SSW-SMC003), International Cooperation Fund of CAS, Shanghai Science and Technology Commission (17ZR1449600, 17ZR1449800), The Pearl River Talent Recruitment Program of Guangdong Province, Shanghai Yangfan Project (16YF1413400, 18YF1427600) and Rising-Star Program (15QA1404300), China Postdoctoral Science Foundation (2016M600337, 2017M611634, 2017M621552, 2016LH0042), China Postdoctoral Innovative Talent Support Program (Juan Tang and Yan Li), China Young Talents Lift Engineering (YESS20160050, 2017QNRC001), AstraZeneca, Boehringer Ingelheim, Sanofi-SIBS Fellowship, Royal Society-Newton Advanced Fellowship (NA170109), Research Council of Hong Kong (04110515, 14111916, C4024-16 W), and Health and Medical Research Fund (03140346, 04152566).

### Disclosures

None.

## REFERENCES

1. Tzahor E, Poss KD. Cardiac regeneration strategies: Staying young at heart. *Science*. 2017;356:1035–1039. doi: 10.1126/science.aam5894
2. Bergmann O, Bhardwaj RD, Bernard S, Zdunek S, Barnabé-Heider F, Walsh S, Zupicich J, Alkass K, Buchholz BA, Druid H, Jovinge S, Frisén J. Evidence for cardiomyocyte renewal in humans. *Science*. 2009;324:98–102. doi: 10.1126/science.1164680

3. Mahmoud AI, Kocabas F, Muralidhar SA, Kimura W, Koura AS, Thet S, Porrello ER, Sadek HA. Meis1 regulates postnatal cardiomyocyte cell cycle arrest. *Nature*. 2013;497:249–253. doi: 10.1038/nature12054
4. Senyo SE, Steinhauser ML, Pizzimenti CL, Yang VK, Cai L, Wang M, Wu TD, Guerquin-Kern JL, Lechene CP, Lee RT. Mammalian heart renewal by pre-existing cardiomyocytes. *Nature*. 2013;493:433–436. doi: 10.1038/nature11682
5. Lin Z, Pu WT. Strategies for cardiac regeneration and repair. *Sci Transl Med*. 2014;6:239rv1. doi: 10.1126/scitranslmed.3006681
6. Segers VF, Lee RT. Stem-cell therapy for cardiac disease. *Nature*. 2008;451:937–942. doi: 10.1038/nature06800
7. Laflamme MA, Murry CE. Regenerating the heart. *Nat Biotechnol*. 2005;23:845–856. doi: 10.1038/nbt1117
8. Beltrami AP, Barlucchi L, Torella D, Baker M, Limana F, Chimenti S, Kasahara H, Rota M, Musso E, Urbanek K, Leri A, Kajstura J, Nadal-Ginard B, Anversa P. Adult cardiac stem cells are multipotent and support myocardial regeneration. *Cell*. 2003;114:763–776. doi: 10.1016/S0092-8674(03)00687-1
9. Ellison GM, Vicinanza C, Smith AJ, Aquila I, Leone A, Waring CD, Henning BJ, Stirparo GG, Papait R, Scarfò M, Agosti V, Viglietto G, Condorelli G, Indolfi C, Ottolenghi S, Torella D, Nadal-Ginard B. Adult c-kit(pos) cardiac stem cells are necessary and sufficient for functional cardiac regeneration and repair. *Cell*. 2013;154:827–842. doi: 10.1016/j.cell.2013.07.039
10. van Berlo JH, Kanisicak O, Maillet M, Vagnozzi RJ, Karch J, Lin SC, Middleton RC, Marbán E, Molkentin JD. c-kit+ cells minimally contribute cardiomyocytes to the heart. *Nature*. 2014;509:337–341. doi: 10.1038/nature13309
11. Sultana N, Zhang L, Yan J, Chen J, Cai W, Razzaque S, Jeong D, Sheng W, Bu L, Xu M, Huang GY, Hajjar RJ, Zhou B, Moon A, Cai CL. Resident c-kit(+) cells in the heart are not cardiac stem cells. *Nat Commun*. 2015;6:8701. doi: 10.1038/ncomms9701
12. Liu Q, Yang R, Huang X, Zhang H, He L, Zhang L, Tian X, Nie Y, Hu S, Yan Y, Zhang L, Qiao Z, Wang QD, Lui KO, Zhou B. Genetic lineage tracing identifies in situ Kit-expressing cardiomyocytes. *Cell Res*. 2016;26:119–130. doi: 10.1038/cr.2015.143
13. He L, Li Y, Li Y, Pu W, Huang X, Tian X, Wang Y, Zhang H, Liu Q, Zhang L, Zhao H, Tang J, Ji H, Cai D, Han Z, Han Z, Nie Y, Hu S, Wang QD, Sun R, Fei J, Wang F, Chen T, Yan Y, Huang H, Pu WT, Zhou B. Enhancing the precision of genetic lineage tracing using dual recombinases. *Nat Med*. 2017;23:1488–1498. doi: 10.1038/nm.4437
14. Valiente-Alandi I, Albo-Castellanos C, Herrero D, Arza E, Garcia-Gomez M, Segovia JC, Capecchi M, Bernad A. Cardiac Bmi1(+) cells contribute to myocardial renewal in the murine adult heart. *Stem Cell Res Ther*. 2015;6:205. doi: 10.1186/s13287-015-0196-9
15. Laugwitz KL, Moretti A, Lam J, Gruber P, Chen Y, Woodard S, Lin LZ, Cai CL, Lu MM, Reth M, Platoshyn O, Yuan JX, Evans S, Chien KR. Postnatal isl1+ cardioblasts enter fully differentiated cardiomyocyte lineages. *Nature*. 2005;433:647–653. doi: 10.1038/nature03215
16. Uchida S, De Gaspari P, Kostin S, Jenniches K, Kilic A, Izumiya Y, Shiojima I, Grosse Kreymborg K, Renz H, Walsh K, Braun T. Sca1-derived cells are a source of myocardial renewal in the murine adult heart. *Stem Cell Reports*. 2013;1:397–410. doi: 10.1016/j.stemcr.2013.09.004
17. Doyle MJ, Maher TJ, Li Q, Garry MG, Sorrentino BP, Martin CM. Abcg2-labeled cells contribute to different cell populations in the embryonic and adult heart. *Stem Cells Dev*. 2016;25:277–284. doi: 10.1089/scd.2015.0272
18. Johnston PV, Sasano T, Mills K, Evers R, Lee ST, Smith RR, Lardo AC, Lai S, Steenbergen C, Gerstenblith G, Lange R, Marbán E. Engraftment, differentiation, and functional benefits of autologous cardiosphere-derived cells in porcine ischemic cardiomyopathy. *Circulation*. 2009;120:1075–83, 7 p following 1083. doi: 10.1161/CIRCULATIONAHA.108.816058
19. Molkentin JD, Houser SR. Are resident c-Kit+ cardiac stem cells really all that are needed to mend a broken heart? *Circ Res*. 2013;113:1037–1039. doi: 10.1161/CIRCRESAHA.113.302564
20. Nadal-Ginard B, Ellison GM, Torella D. Response to Molkentin's letter to the editor regarding article, "the absence of evidence is not evidence of absence: the pitfalls of Cre knock-ins in the c-kit locus." *Circ Res*. 2014;115:e38–9. doi: 10.1161/CIRCRESAHA.115.305380
21. Molkentin JD. Letter by Molkentin regarding article, "The absence of evidence is not evidence of absence: the pitfalls of Cre Knock-Ins in the c-Kit Locus." *Circ Res*. 2014;115:e21–e23. doi: 10.1161/CIRCRESAHA.114.305011
22. Hochedlinger K, Yamada Y, Beard C, Jaenisch R. Ectopic expression of Oct-4 blocks progenitor-cell differentiation and causes dysplasia in epithelial tissues. *Cell*. 2005;121:465–477. doi: 10.1016/j.cell.2005.02.018
23. Perl AK, Wert SE, Nagy A, Lobe CG, Whitsett JA. Early restriction of peripheral and proximal cell lineages during formation of the lung. *Proc Natl Acad Sci U S A*. 2002;99:10482–10487. doi: 10.1073/pnas.152238499
24. Sohal DS, Nghiem M, Crackower MA, Witt SA, Kimball TR, Tymitz KM, Penninger JM, Molkentin JD. Temporally regulated and tissue-specific gene manipulations in the adult and embryonic heart using a tamoxifen-inducible Cre protein. *Circ Res*. 2001;89:20–25. doi: 10.1161/hh1301.092687
25. Zhang H, Pu W, Li G, Huang X, He L, Tian X, Liu Q, Zhang L, Wu SM, Sucov HM, Zhou B. Endocardium minimally contributes to coronary endothelium in the embryonic ventricular free walls. *Circ Res*. 2016;118:1880–1893. doi: 10.1161/CIRCRESAHA.116.308749
26. Wirth A, Benyó Z, Lukasova M, Leutgeb B, Wettschureck N, Gorbey S, Orsy P, Horváth B, Maser-Gluth C, Greiner E, Lemmer B, Schütz G, Gutkind JS, Offermanns S. G12-G13-LARG-mediated signaling in vascular smooth muscle is required for salt-induced hypertension. *Nat Med*. 2008;14:64–68. doi: 10.1038/nm1666
27. He L, Huang X, Kanisicak O, Li Y, Wang Y, Li Y, Pu W, Liu Q, Zhang H, Tian X, Zhao H, Liu X, Zhang S, Nie Y, Hu S, Miao X, Wang QD, Wang F, Chen T, Xu Q, Lui KO, Molkentin JD, Zhou B. Preexisting endothelial cells mediate cardiac neovascularization after injury. *J Clin Invest*. 2017;127:2968–2981. doi: 10.1172/JCI93868
28. Chen Q, Zhang H, Liu Y, Adams S, Eilken H, Stehling M, Corada M, Dejana E, Zhou B, Adams RH. Endothelial cells are progenitors of cardiac pericytes and vascular smooth muscle cells. *Nat Commun*. 2016;7:12422. doi: 10.1038/ncomms12422
29. Wang Y, Nakayama M, Pitulescu ME, Schmidt TS, Bochenek ML, Sakakibara A, Adams S, Davy A, Deutsch U, Lüthi U, Barberis A, Benjamin LE, Mäkinen T, Nobes CD, Adams RH. Ephrin-B2 controls VEGF-induced angiogenesis and lymphangiogenesis. *Nature*. 2010;465:483–486. doi: 10.1038/nature09002
30. Zhu X, Hill RA, Dietrich D, Komitova M, Suzuki R, Nishiyama A. Age-dependent fate and lineage restriction of single NG2 cells. *Development*. 2011;138:745–753. doi: 10.1242/dev.047951
31. Zhou B, Ma Q, Rajagopal S, Wu SM, Domian I, Rivera-Feliciano J, Jiang D, von Gise A, Ikeda S, Chien KR, Pu WT. Epicardial progenitors contribute to the cardiomyocyte lineage in the developing heart. *Nature*. 2008;454:109–113. doi: 10.1038/nature07060
32. Zhang H, Huang X, Liu K, Tang J, He L, Pu W, Liu Q, Li Y, Tian X, Wang Y, Zhang L, Yu Y, Wang H, Hu R, Wang F, Chen T, Wang QD, Qiao Z, Zhang L, Lui KO, Zhou B. Fibroblasts in an endocardial fibroelastosis disease model mainly originate from mesenchymal derivatives of epicardium. *Cell Res*. 2017;27:1157–1177. doi: 10.1038/cr.2017.103
33. Cai CL, Liang X, Shi Y, Chu PH, Pfaff SL, Chen J, Evans S. Isl1 identifies a cardiac progenitor population that proliferates prior to differentiation and contributes a majority of cells to the heart. *Dev Cell*. 2003;5:877–889. doi: 10.1016/S1534-5807(03)00363-0
34. Buckingham M, Meilhac S, Zaffran S. Building the mammalian heart from two sources of myocardial cells. *Nat Rev Genet*. 2005;6:826–835. doi: 10.1038/nrg1710
35. Jiao K, Kulessa H, Tompkins K, Zhou Y, Batts L, Baldwin HS, Hogan BL. An essential role of Bmp4 in the atrioventricular septation of the mouse heart. *Genes Dev*. 2003;17:2362–2367. doi: 10.1101/gad.1124803
36. Soriano P. Generalized lacZ expression with the ROSA26 Cre reporter strain. *Nat Genet*. 1999;21:70–71. doi: 10.1038/5007
37. Corish P, Tyler-Smith C. Attenuation of green fluorescent protein half-life in mammalian cells. *Protein Eng*. 1999;12:1035–1040. doi: 10.1093/protein/12.12.1035
38. Kikuchi K, Holdway JE, Werdich AA, Anderson RM, Fang Y, Egnaczyk GF, Evans T, Macrae CA, Stainier DY, Poss KD. Primary contribution to zebrafish heart regeneration by gata4(+) cardiomyocytes. *Nature*. 2010;464:601–605. doi: 10.1038/nature08804
39. Jopling C, Sleep E, Raya M, Martí M, Raya A, Izpisúa Belmonte JC. Zebrafish heart regeneration occurs by cardiomyocyte dedifferentiation and proliferation. *Nature*. 2010;464:606–609. doi: 10.1038/nature08899
40. Qian L, Huang Y, Spencer CI, Foley A, Vedantham V, Liu L, Conway SJ, Fu JD, Srivastava D. *In vivo* reprogramming of murine cardiac fibroblasts into induced cardiomyocytes. *Nature*. 2012;485:593–598. doi: 10.1038/nature11044
41. Song K, Nam YJ, Luo X, Qi X, Tan W, Huang GN, Acharya A, Smith CL, Tallquist MD, Neilson EG, Hill JA, Bassel-Duby R, Olson EN. Heart repair by reprogramming non-myocytes with cardiac transcription factors. *Nature*. 2012;485:599–604. doi: 10.1038/nature11139
42. Smart N, Bollini S, Dubé KN, Vieira JM, Zhou B, Davidson S, Yellon D, Riegler J, Price AN, Lythgoe MF, Pu WT, Riley PR. De novo cardiomyocytes from within the activated adult heart after injury. *Nature*. 2011;474:640–644. doi: 10.1038/nature10188

43. Furuyama K, Kawaguchi Y, Akiyama H, Horiguchi M, Kodama S, Kuhara T, Hosokawa S, Elbahrawy A, Soeda T, Koizumi M, Masui T, Kawaguchi M, Takaori K, Doi R, Nishi E, Kakinoki R, Deng JM, Behringer RR, Nakamura T, Uemoto S. Continuous cell supply from a Sox9-expressing progenitor zone in adult liver, exocrine pancreas and intestine. *Nat Genet*. 2011;43:34–41. doi: 10.1038/ng.722
44. Yanger K, Knigin D, Zong Y, Maggs L, Gu G, Akiyama H, Pikarsky E, Stanger BZ. Adult hepatocytes are generated by self-duplication rather than stem cell differentiation. *Cell Stem Cell*. 2014;15:340–349. doi: 10.1016/j.stem.2014.06.003
45. Dor Y, Brown J, Martinez OI, Melton DA. Adult pancreatic beta-cells are formed by self-duplication rather than stem-cell differentiation. *Nature*. 2004;429:41–46. doi: 10.1038/nature02520
46. Dor Y, Melton DA. Facultative endocrine progenitor cells in the adult pancreas. *Cell*. 2008;132:183–184. doi: 10.1016/j.cell.2008.01.004
47. Van Keymeulen A, Rocha AS, Ousset M, Beck B, Bouvencourt G, Rock J, Sharma N, Dekoninck S, Blanpain C. Distinct stem cells contribute to mammary gland development and maintenance. *Nature*. 2011;479:189–193. doi: 10.1038/nature10573
48. Rios AC, Fu NY, Lindeman GJ, Visvader JE. In situ identification of bipotent stem cells in the mammary gland. *Nature*. 2014;506:322–327. doi: 10.1038/nature12948
49. Terada N, Hamazaki T, Oka M, Hoki M, Mastalerz DM, Nakano Y, Meyer EM, Morel L, Petersen BE, Scott EW. Bone marrow cells adopt the phenotype of other cells by spontaneous cell fusion. *Nature*. 2002;416:542–545. doi: 10.1038/nature730
50. Wang X, Willenbring H, Akkari Y, Torimaru Y, Foster M, Al-Dhalimy M, Lagasse E, Finegold M, Olson S, Grompe M. Cell fusion is the principal source of bone-marrow-derived hepatocytes. *Nature*. 2003;422:897–901. doi: 10.1038/nature01531